Photoacoustic X-Ray Absorption Fine-Structure Spectroscopy of the Ni K-Edge

M. Reichling[1], T. Masujima[2], H. Shiwaku[2], H. Kawata[3], M. Ando[3], and E. Matthias[1]

1 Institut für Atom- und Festkörperphysik, Freie Universität Berlin,
D-1000 Berlin 33
[2] Institute of Pharmaceutical Sciences, University, Hiroshima 734, Japan
[3] KEK, National Laboratory for High Energy Physics, Ibaraki 305, Japan

Abstract. The X-ray absorption in a 5 μm thick Ni foil for energies from 8.2 keV to 8.8 keV was measured by the photoacoustic method using a gas-microphone-cell. Results are presented for both photoacoustic amplitude and phase as a function of incident photon energy. The absorption fine structure above the Ni K-edge is clearly resolved. The data are compared with a simple theory for the signal generation, and discrepancies are explained by discussing the various energy dissipation channels following the X-ray absorption.

Measuring the extended X-ray absorption fine-structure (EXAFS) has become a standard tool for the determination of structural properties of solids and surfaces [1,2]. The EXAFS-spectrum is usually recorded by either directly measuring the absorption coefficient or by observing secondary processes following the X-ray absorption, i.e. emission of photons or electrons. The fluorescence technique probes bulk properties and is therefore of advantage for thick concentrated samples. However, using a glancing incidence geometry this technique can also be applied to near surface studies [3]. Experimental difficulties arise mainly from self-absorption and scattering effects [4]. Due to the small escape depth of electrons from solids the electron yield technique [5] is also somewhat surface sensitive [6]. However, for measurements of this kind the sample has to be enclosed in a vacuum or in an ionization chamber [7].

There have been several attempts to use photoacoustic (PA) methods for X-ray spectroscopy. After first experiments with pulsed X-rays detected by a piezoelectric transducer [8], the PA dosimetry for soft and hard X-rays was developed [9,10]. In the soft X-ray region a pyroelectric calorimeter has been used for the spectroscopy of the carbon K-edge [11] and organic materials were investigated using the gas-microphone technique [12]. In the latter two experiments synchrotron radiation from an electron storage ring was used. For hard X-rays it is even possible to detect the emission from a X-ray tube [13].

Recently Masujima et al. [14], using high energy synchrotron radiation, have shown that the gas-microphone technique offers an experimentally simple alternative for recording the EXAFS-spectrum. In contrast to more conventional detection schemes the photoacoustic method does not measure emitted particles or radiation but rather the heat deposited in the irradiated sample. The heat results from the thermalization cascade of Auger- and photoelectrons produced by the absorption of X-rays and secondary electrons excited by the reabsorption of X-ray fluorescence in the sample. The surface of the solid target is in contact with a gas cell, and here the heat is converted into an acoustic wave which, in turn, is recorded by a microphone. This photoacoustic technique is related to the above-mentioned methods, electron yield and fluorescence detection. The main difference is that instead of the outgoing photons or electrons it records the integrated energy that remains in the sample. Consequently, the photoacoustic X-ray absorption spectroscopy (PAXAS) is complementary to electron and fluorescence detection.

Like most of the photoacoustic sensing techniques [15] it provides the possibility of depth profiling by adjusting experimental parameters to the thermal properties of the material under investigation. In experiments with chopped beams, as introduced here, the chopping frequency will determine whether near surface regions or bulk properties are probed. By monitoring the phase of the photoacoustic signal it is possible to identify the effective energy absorption depth profile [16]. For a quantitative interpretation of photoacoustic data it is first of all necessary to model the energy relaxation processes following the initial excitation of core electrons. According to model calculations for the photoacoustic response of molecular systems irradiated by visible light [17], the transition rates of the main radiative and radiationless channels have to be included. If the chopping frequency is low compared to the transition rates, as is the case for our measurements, the dynamics of the relaxation can be neglected and the process may be described in terms of two overall probabilities for fluorescence and radiationless deexcitation. An initial theoretical attempt in this direction by Garcia et al. [18] yields reasonable agreement with experiments on the copper K-edge for amplitude spectra. It suffers from the drawback, however, that the energy deposition profile was taken to be an exponential function of depth, and completely ignores energy losses by reemission near the surfaces. Hence, it is fair to say that the process of photoacoustic signal generation after X-ray excitation is presently still not understood in full detail and several questions remain to be answered about the details of the energy dissipation channels.

In this paper we present the amplitude and phase spectra of photoacoustic EXAFS at the Ni K-edge. The experimental data are compared with theoretical curves calculated using the formalism of Garcia et al. [18] combined with the standard photoacoustic response theory of Rosencwaig and Gersho [19]. The measurements were performed at beamline 14 A at the Photon Factory of the KEK National Laboratory for High Energy Physics, Japan. The monochromator provides a beam of tunable X-ray radiation with an intensity of 10^9 to 10^{10} photons/s. The experimental arrangement is shown in the inset of Fig. 1. The X-ray beam is chopped with a frequency of 11.2 Hz and passes a first ion chamber to monitor the incoming photon flux. Then the beam penetrates the photoacoustic (PA) cell containing the sample which, in our case, is a polycrystalline 5 μm Ni foil placed in front of the exit Be window. Details of the PA cell are described elsewhere [20]. The transmitted X-rays are measured by a second ion chamber, providing a conventional absorption spectrum. Detected by a lock-in amplifier, the photoacoustic signals together with wavelength
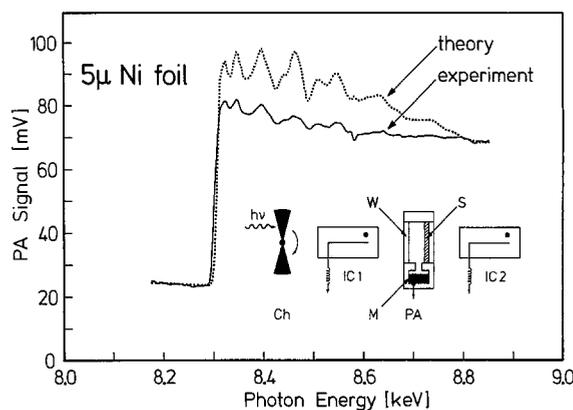
Fig. 1. Photoacoustic EXAFS of a 5 μm Ni foil. Solid curve: measured PA amplitude, dotted curve: PA amplitude calculated from simple theory. Inset: experimental setup with Ch: chopper, IC 1/2: ion chambers, PA: photoacoustic cell, M: microphone, W: Be window, S: sample

data and corresponding ion chamber currents are processed by a microcomputer that calculates the amplitude and phase spectrum. After background subtraction, the PA amplitude is normalized with respect to the current of the first ion chamber and data are corrected for the energy dependent absorption in the chamber. The small path absorptions in the air and the Be windows are also taken into account in the data analysis.

The solid curve in Fig. 1 shows the measured PA-signal as a function of photon energy. The edge structure is clearly resolved for energies up to about 400 eV above the edge. The Fourier transform of the EXAFS-oscillations is in good agreement with the absorption data not shown here. However, in the photoacoustic case the amplitude compared to the edge-jump is smaller by a factor of two. This observation might be of the same origin as the damped oscillation amplitude observed in electron yield spectra [6].

The main new feature introduced by the PA method is the phase spectrum shown in Fig. 2. The phase has a constant value of $-45°$ for energies below the edge as expected for a thermally and optically thin sample [19]. After the edge-jump of about 3° the phase then shows a smooth variation with energy to reach a saturation value of $-53°$ at about 500 eV above the edge. A very similar phase spectrum was obtained with a 5 μm Cu foil. However, for thicker samples (e.g. 20 μm Ni foil) a larger edge jump is observed and the phase remains at a constant value within the experimental uncertainty for all energies above the edge. We conclude that the phase variation above the edge is a special feature of thin samples resulting from energy loss near surfaces and the redistribution of energy by
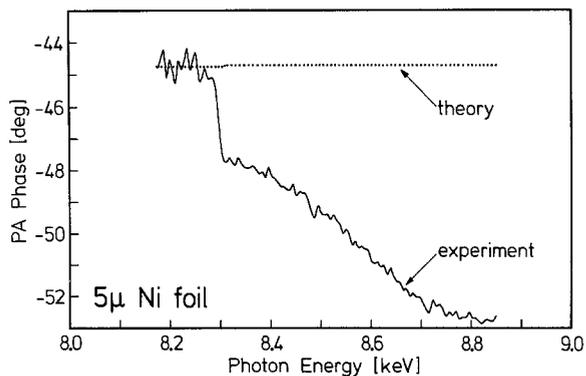
Fig. 2. Photon energy dependent phase for photoacoustic EXAFS of a 5 µm Ni foil. Solid curve: measured PA phase, dotted curve: PA phase calculated from simple theory

secondary emission and reabsorption, which clearly plays a minor role in thick samples. Hence, a systematic study of the phase spectra as a function of sample thickness in future experiments will certainly contribute to a better understanding of the processes involved in the PA signal generation.

The phase is a sensitive parameter for testing model calculations. tions. A good illustration of this point are the results of a simple calculation outlined in the following. Let us consider the sequence of secondary processes that are relevant for the X-ray induced photoacoustic signal generation. Those are (1) Auger decay and X-ray fluorescence, (2) subsequent reabsorption of fluorescence photons and thermalization of excited electrons, and (3) the dissipation of the produced heat and conversion into acoustic energy. For the description of the first two steps we use the algorithm given by Garcia et al. [18] in order to derive an efficiency parameter $\varepsilon(\hbar\omega)$ for the energy conversion of the absorbed photon energy into heat. Here, ε is defined as the fraction of energy $S(\hbar\omega)$ that is thermalized divided by the total absorbed energy:

$$\varepsilon(\hbar\omega) = S(\hbar\omega)/[\hbar\omega(1 - e^{-\mu(\hbar\omega)d})] , \qquad (1)$$

where $\hbar\omega$ is the energy of the incident photons, $\mu(\hbar\omega)$ is the absorption coefficient and d the sample thickness. The important parameters that determine ε besides wavelength and absorption of incoming photons are the Auger and fluorescence energies and probabilities for fluorescence deexcitation of the sample material.

To describe the PA signal generation we use the standard theory of Rosencwaig and Gersho [19] who calculate the acoustic intensity $Q(\hbar\omega)$ for a given incoming photon flux $I_0(\hbar\omega)$. Q is controlled by thermal parameters, the absorption coefficient of the sample and by the chopping frequency. As we use thin samples with high thermal conductivity and a low chopping frequency, heat losses via the backing

material may not be neglected and the thermal properties of the rear Be windows have to be included [19]. Combining all quantities one finds for the normalized photoacoustic signal $PA(\hbar\omega)$ the relation:

$$PA(\hbar\omega) = \varepsilon(\hbar\omega)Q(\hbar\omega)/I_0(\hbar\omega) = |PA(\hbar\omega)|e^{i\phi(\hbar\omega)} . \qquad (2)$$

The magnitude and phase of $PA(\hbar\omega)$ are plotted as dotted curves in Figs. 1 and 2 respectively and may be directly compared to the experimental data. The theoretical values for the PA amplitude are multiplied by a scaling factor to achieve normalization to the experimental data for energies below the absorption edge. Summarizing the results from different measurements there is no convincing agreement between this theory and our experimental data for energies above the K-absorption edge. Especially the observed phase behavior is completely different from the theoretical predictions. For the 5 µm Ni sample (Fig. 2) the calculated phase jump is only one tenth of a degree towards a smaller phase lag which appears to be a plausible result from simple heat diffusion theory. An increase in absorption means a slight shift of heat production towards the surface. Consequently, during diffusion the heat is expected to need less time to reach the surface and produce the acoustic signal, resulting in a smaller phase lag [21]. However, the measured phase change is several degrees in the opposite direction.

The discrepancies between predicted and observed amplitude and phase can be explained qualitatively by considering some of the energy loss and energy redistribution mechanisms that are not covered by the simple theory. The starting point of Rosencwaig and Gersho [19] is an exponential decay of light intensity inside the sample. The thermalization process will be fast and localized. Hence the heat production profile is assumed to be described by the same exponential as the absorption law and the PA signal phase is only dependent on the thermal diffusion. In the X-ray case this is true for energies below the K-edge. Due to the small fluorescence yield for L-shell excitations in Ni [22], 99% of the energy is transferred to photo- and Auger-electrons whose thermalization length is small compared to the diffusion length ($\simeq 1$ mm) and to the sample dimensions. The situation changes drastically above the K-edge. In the case of Ni about 40% of the absorbed energy will be released in form of fluorescence radiation [22]. For a 5 µm sample, however, the absorption length of these secondary X-rays ($\simeq 5$–20 µm) [23] is comparable to the foil thickness. Therefore, a considerable fraction of fluorescence radiation will leave the sample, in particular from the near surface regions, and will be lost for heat production. The other part is reabsorbed in deeper regions and converted there to heat. Of course, there will also

be some energy transfer from the rear to the front of the foil. However, as a consequence of the exponential absorption profile of the primary X-rays and the reabsorption of fluorescence photons in the backing material, the net effect will be a shift of heat production towards the middle of the sample, and thus a greater delay of the photoacoustic signal, compared to the Rosencwaig and Gersho assumption. For the same reason one also expects a lateral energy spread leading to a decrease in the PA amplitude.

For thin samples the emission of electrons must also be taken into account. Using the experimental results and the semi-empirical formula for the electron escape depth given by Elam et al. [7], we assume an escape depth of 0.2 μm for Ni KLL-Auger electrons. This means that at least 3% of the total absorbed energy will be lost by electron emission from the front surface of a 5 μm sample. The electrons emitted from the rear surface will be completely reabsorbed by the Be backing and produce heat there. The result is again an energy transfer in the same direction as for the reabsorbed fluorescence.

With the above considerations in mind, the experimental facts can be understood. The edge-jump of the PA amplitude is somewhat lower than expected because theory neglects the emission of electrons and over-estimates fluorescence reabsorption. Due to the shift of heat production towards the center of the sample for energies above the K-edge, the phase lag of the PA signal increases for increasing energies as evidenced by the data in Fig. 2. Since the phase shift is partially caused by near-surface effects, these observations are dominant in spectra of very thin foils and are less prominent for thicker samples.

In conclusion we have shown that amplitude and phase spectra of the presented PAXAS measurements are not only governed by thermal diffusion but that fluorescence reabsorption and Auger electron emission must be taken into consideration. Experiments of the kind presented here are capable of revealing information about the depth profile of the effective energy absorption. To achieve a full understanding of all features in the spectra a theory is needed which simulates all different energy dissipation channels and the acoustic signal production in a three dimensional model. Such a theory would be especially important for the interpretation of the phase shifts which are the key to a further development of the PAXAS method.

References

1. B.K. Teo: *EXAFS: Basic Principles and Data Analysis* (Springer, Berlin, Heidelberg 1986)
2. D.C. Koningsberger, R. Prins (eds.): *X-Ray Absorption* (Wiley, New York 1988)
3. S.M. Heald, E. Keller, E.A. Stern: Phys. Lett. **103A**, 155 (1984)
4. J. Baines, C.D. Garner, S.S. Hasnain, C. Morrell: J. Physique, Coll. C**8**, Suppl. 12 (47), C8–163 (1986)
5. G. Martens, P. Rabe, N. Schwentner, A. Werner: J. Phys. C **11**, 3125 (1978)
6. T. Guo, M.L. den Boer: Phys. Rev. B **31**, 6233 (1985)
7. W.T. Elam, J.P. Kirkland, R.A. Neiser, P.D. Wolf: Phys. Rev. B **38**, 26 (1988)
8. K.Y. Kim, W. Sachse: Appl. Phys. Lett. **43**, 1099 (1983)
9. R. Germer: Rev. Sci. Instrum. **55**, 1461 (1984)
10. S. Mascarenhas, H. Vargas, C.L. Cesar: Med. Phys. **11**, 73 (1984)
11. H. Coufal, J. Stöhr, K. Baberschke: Springer Ser. Opt. Sci., Vol. 58, ed. by P. Hess, J. Pelzl (Springer, Berlin, Heidelberg 1988) p. 25
12. T. Inagaki, Y. Furusawa, K. Hieda, H. Maezawa, T. Ito: Springer Ser. Opt. Sci., Vol. 58, ed. by P. Hess, J. Pelzl (Springer, Berlin, Heidelberg 1988) p. 29
13. Y. Sugitani, S. Aoki, K. Kato, Y. Kobayashi: Springer Ser. Opt. Sci., Vol. 58, ed. by P. Hess, J. Pelzl (Springer, Berlin, Heidelberg 1988) p. 31
14. T. Masujima et al.: Chem. Lett. 1987, 973 and T. Masujima: Springer Ser. Opt. Sci., Vol. 58, ed. by P. Hess, J. Pelzl (Springer, Berlin, Heidelberg 1988) p. 19
15. A.C. Tam: Rev. Mod. Phys. **58**, 381 (1986)
16. T. Masujima: In Topics Curr. Chem., Vol. II, ed. E. Mandelkow (Springer, Berlin, Heidelberg 1989)
17. E. Hey, K. Gollnick: J. Photoacoust. **1**, 1 (1982)
18. M.E. Garcia, G.M. Pastor, K.H. Bennemann: Phys. Rev. Lett. **61**, 121 (1988)
19. A. Rosencwaig, A. Gersho: J. Appl. Phys. **7**, 64 (1976)
20. E.M. Eyring, J.J. Komorowski, T. Masujima: *Analytical Instrumentation Handbook*, ed. by G. Ewing (Dekker, New York 1988)
    T. Masujima et al.: Instrumentation for Photoacoustic EXAFS Method, Rev. Sci. Instr. (to be published)
21. J. Opsal, A. Rosencwaig: J. Appl. Phys. **53**, 4240 (1982)
22. M.O. Krause: J. Phys. Chem. Ref. Data **8**, 307 (1979)
23. International Tables for X-ray Crystallography, ed. by K. Lonsdale (The Kynoch Press, Birmingham 1962)